

## $G\beta\gamma$ -dependent and $G\beta\gamma$ -independent Basal Activity of G Protein-activated $K^+$ Channels\*

Received for publication, October 27, 2004, and in revised form, February 22, 2005  
Published, JBC Papers in Press, February 23, 2005, DOI 10.1074/jbc.M412196200

Ida Rishal, Yuri Porozov, Daniel Yakubovich, Dalia Varon, and Nathan Dascal‡

From the Department of Physiology and Pharmacology, Sackler School of Medicine, Tel Aviv University, Ramat Aviv 69978, Israel

Cardiac and neuronal G protein-activated  $K^+$  channels (GIRK; Kir3) open following the binding of  $G\beta\gamma$  subunits, released from  $G_{i/o}$  proteins activated by neurotransmitters. GIRKs also possess basal activity contributing to the resting potential in neurons. It appears to depend largely on free  $G\beta\gamma$ , but a  $G\beta\gamma$ -independent component has also been envisaged. We investigated  $G\beta\gamma$  dependence of the basal GIRK activity ( $A_{GIRK,basal}$ ) quantitatively, by titrated expression of  $G\beta\gamma$  scavengers, in *Xenopus* oocytes expressing GIRK1/2 channels and muscarinic m2 receptors. The widely used  $G\beta\gamma$  scavenger, myristoylated C terminus of  $\beta$ -adrenergic kinase (m-c $\beta$ ARK), reduced  $A_{GIRK,basal}$  by 70–80% and eliminated the acetylcholine-evoked current ( $I_{ACh}$ ). However, we found that m-c $\beta$ ARK directly binds to GIRK, complicating the interpretation of physiological data. Among several newly constructed  $G\beta\gamma$  scavengers, phosducin with an added myristoylation signal (m-phosducin) was most efficient in reducing GIRK currents. m-phosducin relocated to the membrane fraction and did not bind GIRK. Titrated expression of m-phosducin caused a reduction of  $A_{GIRK,basal}$  by up to 90%. Expression of GIRK was accompanied by an increase in the level of  $G\beta\gamma$  and  $G\alpha$  in the plasma membrane, supporting the existence of preformed complexes of GIRK with G protein subunits. Increased expression of  $G\beta\gamma$  and its constitutive association with GIRK may underlie the excessively high  $A_{GIRK,basal}$  observed at high expression levels of GIRK. Only 10–15% of  $A_{GIRK,basal}$  persisted upon expression of both m-phosducin and c $\beta$ ARK. These results demonstrate that a major part of  $I_{basal}$  is  $G\beta\gamma$ -dependent at all levels of channel expression, and only a small fraction (<10%) may be  $G\beta\gamma$ -independent.

G protein-activated, inwardly rectifying  $K^+$  channels (GIRK, Kir3)<sup>1</sup> mediate postsynaptic inhibitory effects of various neu-

rotransmitters in the brain and atrium via seven-helix, G protein-coupled receptors (GPCRs) linked to pertussis toxin-sensitive G proteins of the  $G_{i/o}$  family. Opening of the channels is the result of a direct binding of  $G\beta\gamma$  subunits released from the  $G\alpha_{i/o}\beta\gamma$  heterotrimers (1–4). The channel can also be activated by cytosolic  $Na^+$  and membranal phosphatidylinositol 4,5-bisphosphate ( $PIP_2$ ); the latter is essential for proper GIRK gating by both  $Na^+$  and  $G\beta\gamma$  (3, 5, 6).

Whereas the physiological role of neurotransmitter-induced GIRK activity is well established, the basal activity of these channels ( $A_{GIRK,basal}$ ) is often regarded as negligible and physiologically unimportant. This feature distinguishes GIRK from many other  $K^+$  channels of the Kir family, such as Kir1 and Kir2, which show high intrinsic activity under physiological conditions and are often referred to as “constitutively active.” Low  $A_{GIRK,basal}$  is supposed to ensure high signal-to-noise ratio for GIRK-related neurotransmitter signaling and to minimize participation of GIRK in resting membrane  $K^+$  conductance (see Ref. 2). However, some classical and many recent studies challenge this concept. In sinoatrial node cells, GIRK channels may contribute a major part of basal  $K^+$  conductance (7). Recent studies in intact neurons indicate that basal activity of GIRK may substantially contribute to resting  $K^+$  conductance, shunting the excitatory postsynaptic potentials and reducing the responses to glutamate (8). Substantial  $A_{GIRK,basal}$  has been reported in hippocampal pyramidal cells (9, 10) and in rat locus coeruleus slices (11). In murine locus coeruleus, where GIRKs mediate most of the inhibitory effects of opioids, knock-out of GIRK subunit genes depolarizes the cell’s resting potential by as much as 20 mV (8). In many cases, it was not clear whether the GIRK activity observed in resting cells under a variety of experimental conditions was a truly agonist-independent one or depended on the presence of “ambient” neurotransmitters or local hormones. For instance, in hippocampal pyramidal cells, one report assigned to ambient adenosine a major role in sustaining most of  $A_{GIRK,basal}$  (9), whereas another one contended that  $A_{GIRK,basal}$  was independent of adenosine or other neurotransmitters (10). In any case, it appears that GIRK plays a substantial role in determining the resting membrane potential at least in some neurons and in sinoatrial pacemaker cells. It is therefore conceivable that not only activation of GIRK by  $G_{i/o}$  coupled neurotransmitters, but also its inhibition by neurotransmitters that activate  $G\alpha_q$  (12–16) may serve as an important mechanism of regulation of neuronal excitability. These considerations urge for a better understanding of the mechanisms of regulation of  $A_{GIRK,basal}$ .

An important contributor to  $A_{GIRK,basal}$  is ambient free  $G\beta\gamma$ . This has been shown in heterologous expression systems; co-

\* This work was supported by National Institutes of Health Grant RO1 GM68493 and USA-Israel Binational Science Foundation Grant 2001-122. The costs of publication of this article were defrayed in part by the payment of page charges. This article must therefore be hereby marked “advertisement” in accordance with 18 U.S.C. Section 1734 solely to indicate this fact.

‡ To whom correspondence should be addressed: Dept. of Physiology and Pharmacology, Sackler School of Medicine, Tel Aviv University, Ramat Aviv 69978, Israel. Tel.: 972-3-6405743; Fax: 972-3-6409113; E-mail: dascaln@post.tau.ac.il.

<sup>1</sup> The abbreviations used are: GIRK, G protein-activated  $K^+$  channel; ACh, acetylcholine;  $A_{GIRK,basal}$ , the basal activity of the GIRK channel;  $I_{basal}$ , the basal activity of GIRK measured in whole oocytes in a high  $K^+$  solution;  $I_{ACh}$ , the ACh-evoked GIRK response; 5HT, 5-hydroxytryptamine (serotonin); aa, amino acid(s); GST, glutathione S-transferase; GPCR, G protein-coupled receptor; m2R, muscarinic receptor type 2; PM, plasma membrane;  $PIP_2$ , phosphatidylinositol 4,5-bisphosphate; m-c $\beta$ ARK, myristoylated C terminus of  $\beta$ -adrenergic

kinase; m-phosducin, phosducin with an added myristoylation signal; n-phosducin, nonmyristoylated phosducin; CHAPS, 3-[(3-cholamidopropyl)dimethylammonio]-1-propanesulfonic acid.

expression of G $\alpha$  subunits and a myristoylated C-terminal segment of  $\beta$ -adrenergic receptor kinase (m-c $\beta$ ARK), used in the past as standard G $\beta\gamma$  scavengers in GIRK studies (17–22), has been reported to reduce  $A_{\text{GIRK,basal}}$  to different extents, between 50 and 90%. It is not clear whether the remaining activity is G $\beta\gamma$ -independent or simply reflects insufficient G $\beta\gamma$  sequestration, leaving open the question of whether a G $\beta\gamma$ -independent  $A_{\text{GIRK,basal}}$  exists. Such G $\beta\gamma$ -independent basal activity could be due to a direct activation by cytosolic free Na<sup>+</sup> (23–25) and/or reflect an intrinsic G $\beta\gamma$ - and Na<sup>+</sup>-independent channel activity. The variability of the reported results regarding the extent of inhibition of  $A_{\text{GIRK,basal}}$  by G $\beta\gamma$  scavengers calls for a better quantitative assessment of the G $\beta\gamma$ -dependent component. Furthermore, the use of G $\alpha$  as a G $\beta\gamma$  scavenger is problematic. Coexpressed G $\alpha_i$  subunits may affect the level of channel expression (20); they interact with GIRK itself and have been hypothesized to affect the gating directly (20, 26–28). This greatly complicates the interpretation of G $\beta\gamma$ -scavenging effects of G $\alpha$  subunits. It is not known whether m-c $\beta$ ARK, widely used to study modulation of ion channels by G $\beta\gamma$  (19, 20, 29–31), directly interacts with GIRKs or affects their expression. Therefore, further study is needed to reliably estimate the G $\beta\gamma$ -dependent part of  $A_{\text{GIRK,basal}}$ .

An intriguing phenomenon related to  $A_{\text{GIRK,basal}}$  has been discovered in *Xenopus* oocytes (20). At low expression levels (densities) of GIRK,  $A_{\text{GIRK,basal}}$  is low, and activation by agonist and by purified G $\beta\gamma$  (in whole cells and in excised patches, respectively) is strong, as expected. However, when more GIRK channels are expressed, their basal activity becomes excessively large at the expense of agonist- or G $\beta\gamma$ -evoked activity. Coexpression of a G $\alpha_i$  subunit restores the normal gating pattern, with low  $A_{\text{GIRK,basal}}$  and high agonist- or G $\beta\gamma$ -evoked activity. We proposed that  $A_{\text{GIRK,basal}}$  is controlled by a number of factors, most prominently G $\beta\gamma$  and G $\alpha$ , and that the balance between these factors collapses when the channel is expressed at high levels in *Xenopus* oocytes, partly because of a lack of G $\alpha$  (20, 28). The excessively high  $A_{\text{GIRK,basal}}$  at high levels of GIRK expression remained incompletely understood. Theoretically, it seemed possible that at high densities GIRK behaves as a constitutively active channel.

To better understand the fundamental mechanisms of  $A_{\text{GIRK,basal}}$ , we have initiated a systematic study of G $\beta\gamma$  dependence of  $A_{\text{GIRK,basal}}$  in *Xenopus* oocytes at different levels of GIRK expression. This heterologous expression system is superior to others for quantitative studies, since it allows both a controlled expression of proteins in very wide ranges and an accurate measurement of expressed proteins in the whole cell and in the plasma membrane (PM). Titrated expression of m-c $\beta$ ARK and a novel membrane-targeted G $\beta\gamma$  scavenger, myristoylated phosducin (m-phosducin), revealed that at least 90% of  $A_{\text{GIRK,basal}}$  is G $\beta\gamma$ -dependent at all levels of expression of GIRK. G $\beta\gamma$ -independent activity, if any, constitutes only a small fraction of  $A_{\text{GIRK,basal}}$ . The excessively high basal activity observed at high levels of channel expression may be due to a constitutive association of GIRK with G $\beta\gamma$ , in the absence of sufficient G $\alpha$  needed to preserve low  $A_{\text{GIRK,basal}}$ .

#### EXPERIMENTAL PROCEDURES

**cDNA Constructs and RNA**—The coding sequences of all cDNAs used in this study for preparation of RNA were inserted into high expression oocyte vectors containing 5'- and 3'-untranslated sequences of *Xenopus*  $\beta$ -globin: pGEMHE or its derivative pGEMHJ or pBS-MXT, as described in our previous publications (12, 32), unless stated otherwise. All PCR-derived cDNAs were sequenced in full at the Tel Aviv University sequencing facility. The original cDNAs of human m2R, human 5HT-1A receptor, mouse GIRK2, rat m-c $\beta$ ARK (aa 452–689<sub>end</sub>) (12, 32), human  $\beta$ ARK (GB X61157), and bovine phosducin (GB M33529) were

kindly provided by E. Peralta, P. Hartig, P. Kofuji, E. Reuveny, R. J. Lefkowitz, and M. Lohse, respectively.

PCR-derived full-length coding sequence of wild type phosducin was inserted into the EcoRI restriction site of pGEMHJ, creating the template for RNA synthesis and expression of wild-type, nonmyristoylated phosducin (n-phosducin). To create a membrane-attached derivative of phosducin, we first constructed a new vector, pGEMHE-myr, on the basis of the pGEMHE vector (33) modified by E. Reuveny, using standard PCR techniques. A DNA sequence, atggggagtagcaagagcaagcctaag-gaccacagccagccgcccgg, was inserted between SmaI and EcoRI restriction sites of the pGEMHE vector. On the protein level, this adds the first 15 N-terminal aa of Src, MGSSKSKPKDPSQRR (34), followed by Glu-Phe (encoded by the nucleotide sequence of the EcoRI site), to any proteins whose coding sequence is inserted between EcoRI and any one of the following restriction sites of pGEMHE polylinker. PCR product corresponding to the entire coding sequence of bovine phosducin, flanked by EcoRI and HindIII, was inserted into the respective restriction sites of pGEMHE-myr.

cDNA for nonmyristoylated C terminus of human  $\beta$ ARK1, n-c $\beta$ ARK, was created by inserting the cDNA sequence encoding aa 460–689<sub>end</sub> of  $\beta$ ARK, preceded by a methionine, flanked by EcoRI and HindIII restriction sites, into the pGEMHJ vector. The comparison of physiological effects of m-c $\beta$ ARK (rat) and n-c $\beta$ ARK (human) is justified by high homology between these proteins (97% identity). To create the fusion proteins m2R-c $\beta$ ARK, 5HT1A-c $\beta$ ARK, and 5HT1A-1TMD-c $\beta$ ARK, PCR-derived coding sequences of m2R, 5HT1A receptor (5HT1AR), and aa 1–67 of 5HT1AR, respectively, flanked by EcoRI restriction sites, were inserted in frame just prior to the n-c $\beta$ ARK sequence made as described above. Point mutations in m-c $\beta$ ARK were done using the QuikChange site-directed mutagenesis kit (Stratagene).

RNA was synthesized *in vitro* using a protocol that ensures incorporation of the GTP cap mainly into the 5' portion of the RNA (35) rather than along the whole length as with commercially available kits. Accordingly, the resulting RNAs are usually more efficient than those obtained by other standard protocols.<sup>2</sup> Unless indicated otherwise, RNAs were injected into the oocytes in the following amounts: m2R, 0.5 ng/oocyte; n-c $\beta$ ARK, m2R-c $\beta$ ARK, 5HTA1-c $\beta$ ARK, 5HTA1-1TMD-c $\beta$ ARK, and m-c $\beta$ ARK<sub>R587Q</sub>, 5 ng/oocyte; n-phosducin, 10 ng/oocyte.

**Xenopus Oocytes Preparation and Electrophysiology**—*Xenopus* oocytes were prepared as described (12, 32), injected with RNA, and incubated for 3–4 days in ND-96 solution (NaCl, 96 mM; KCl, 2 mM; CaCl<sub>2</sub>, 1 mM; MgCl<sub>2</sub>, 1 mM; Hepes/NaOH, 5 mM, pH 7.6) supplemented with gentamycin (50  $\mu$ g/ml) and sodium pyruvate (2.5 mM). All experiments were done at 20–22 °C. Whole-cell GIRK currents were measured using a two-electrode voltage clamp with OC-725B (Warner Instruments Corp.), using agarose cushion electrodes (36) filled with 3 M KCl, with resistances of 0.1–0.5 megaohms. Oocytes were held at –80 mV in the ND-96 solution, and GIRK currents were measured in high K<sup>+</sup> solutions, high K 96 or high K 24. High K 96 contained 96 mM KCl, 2 mM NaCl, 1 mM CaCl<sub>2</sub>, 1 mM MgCl<sub>2</sub>, 5 mM Hepes (pH 7.5). High K 24 contained 24 mM KCl, 72 mM NaCl, 1 mM CaCl<sub>2</sub>, 1 mM MgCl<sub>2</sub>, 5 mM Hepes (pH 7.5). Data acquisition and analysis were done using Axotape and pCLAMP software (Axon Instruments Inc., Foster City, CA).

Interaction between GST fusion proteins and phosducin and c $\beta$ ARK was studied as described (21). Briefly, GST-CT-GIRK1 fusion protein was purified, and its interaction with [<sup>35</sup>S]methionine-labeled proteins (the various forms of c $\beta$ ARK, phosducin, and G $\beta_1\gamma_2$ ) synthesized in rabbit reticulocyte lysate (Promega) was monitored using a standard pull-down procedure. GST-GIRK1-CT or GST-GIRK1-NT (5–10  $\mu$ g) was incubated for 1 h with 5  $\mu$ l of reticulocyte lysate containing the designated [<sup>35</sup>S]methionine-labeled proteins in 300  $\mu$ l of a high K<sup>+</sup> buffer (150 mM KCl, 50 mM Tris, 5 mM MgCl<sub>2</sub>, 1 mM EDTA, pH 7.0) with the addition of 0.5% CHAPS. Then 30  $\mu$ l of glutathione-Sepharose beads (Amersham Biosciences) were added, and the mixture was incubated for 30 min at 4 °C and washed in 1 ml of the same buffer (once with 0.5% and twice with 0.1% CHAPS). Bound proteins were eluted with 30  $\mu$ l of 15 mM reduced glutathione and analyzed on 12% SDS-polyacrylamide gels. The labeled products were imaged and quantified by autoradiography using a PhosphorImager (Amersham Biosciences).

**Western Blot Analysis**—The oocytes were homogenized on ice in homogenization buffer (20 mM Tris, pH 7.4, 5 mM EGTA, 5 mM EDTA, and 100 mM NaCl) containing the Roche Applied Science protease inhibitor mixture. Debris was removed by centrifugation twice at 1000  $\times$  g for 15 min at 4 °C. Total cellular membrane fraction from 5–17 oocytes was obtained by 1 h of ultracentrifugation at 100,000  $\times$  g. For

<sup>2</sup> N. Dascal, unpublished observations.

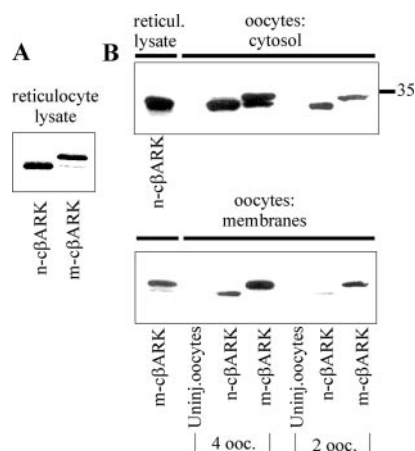


**FIG. 1. Myristoylation helps c $\beta$ ARK to associate with membranes.** *A*, autoradiogram of n-c $\beta$ ARK and m-c $\beta$ ARK expressed in reticulocyte lysate. *B*, Western blot of n-c $\beta$ ARK and m-c $\beta$ ARK expressed in oocytes (*ooc.*) and in reticulocyte lysate. Cytosolic (*top panel*) and membrane (*bottom panel*) fractions of oocytes were separated by differential centrifugation (100,000  $\times$  *g*). m-c $\beta$ ARK was preferentially targeted to the membrane fraction.

Western blots, protein samples were separated on SDS-12% polyacrylamide gels. Antibodies against c $\beta$ ARK, phosducin, and G $\beta$  common (Santa Cruz Biotechnology, Inc., Santa Cruz, CA) were used. Visualization of protein bands was performed using ECL reagents obtained from Pierce. The intensity of labeling was quantified using TINA software (Raytest, Straubenhardt, Germany).

**Confocal Imaging of GIRK, G $\alpha$ , and G $\beta$  in Plasma Membrane**—The levels of expressed proteins in PM were measured as described (20, 37). Briefly, large oocyte membrane patches were attached to coverslips with their cytoplasmic leaflet facing the external solution; fixed; stained by 0.75 ng/ $\mu$ l of a specific GIRK1 antibody (Alomone Laboratories, Jerusalem), 0.5 ng/ $\mu$ l of a common G $\beta$  antibody (Santa Cruz Biotechnology), or 2.5 ng/ $\mu$ l of a common G $\alpha$  antibody (Calbiochem); and visualized using a Cy3-conjugated rabbit IgG (Jackson Immunoresearch Laboratories) using a Zeiss LSM 410 or a Leica TCS SP2 confocal microscope. Intensity of labeling (OD units) was measured with TINA software. In control experiments (Fig. 8, *A* and *B*), to estimate the specificity of labeling by the G $\alpha$  and G $\beta$  antibodies, purified G $\alpha_{i1}$ -GDP or purified G $\beta_{1\gamma_2}$ , respectively, was added in 20-fold excess (w/w) over the antibodies. The purified G $\alpha_{i1}$  and G $\beta_{1\gamma_2}$  were a generous gift from C. W. Dessauer (University of Texas, Houston).

**Data Presentation and Statistics**—Data are presented as mean  $\pm$  S.E. Comparison between two groups of treatment was done using the two-tailed Student's *t* test. Comparisons among several groups of data have been performed using one-way analysis of variance followed by Dunnett's test. The level of statistical significance is indicated in the figures as follows: \*, *p* < 0.05; \*\*, *p* < 0.01; \*\*\*, *p* < 0.001.

## RESULTS

**m-c $\beta$ ARK Reduces  $I_{\text{basal}}$  but It Also Binds to the C Terminus of the GIRK1 Subunit**—To separate the G $\beta$ -dependent component of  $A_{\text{GIRK, basal}}$ , we have initially utilized the widely used G $\beta$  scavenger, m-c $\beta$ ARK. GIRK activation by G $\beta$  is membrane-delimited (1), so that only PM-attached G $\beta$  can activate the channel. Targeting of m-c $\beta$ ARK to the membranes is provided by the myristoylation signal (the first 15 aa of Src added to the N terminus of m-c $\beta$ ARK) (29, 34). For comparison, we have also constructed and tested a nonmyristoylated c $\beta$ ARK (n-c $\beta$ ARK), which should not be targeted to the membrane and thus is supposed to be less efficient than m-c $\beta$ ARK in inhibiting GIRK. As shown in Fig. 1, both m-c $\beta$ ARK and n-c $\beta$ ARK were well expressed in reticulocyte lysate (Fig. 1*A*) and in oocytes (Fig. 1*B*). m-c $\beta$ ARK showed two characteristic bands on SDS gels (Fig. 1, *A* and *B*). The lower band probably corresponded to the presence of a fraction of protein that remained nonmyristoylated, since only the upper band was present in the total membrane fraction (Fig. 1*B*, *bottom*). Only a small proportion of n-c $\beta$ ARK was found in the membrane fraction. Myristoyla-

tion of m-c $\beta$ ARK appeared to be more efficient in reticulocyte lysate than in the oocytes (Fig. 1, compare *A* and *B*). m-c $\beta$ ARK ran on the gel shown in this figure below the 35-kDa molecular size marker, but its actual molecular size was closer to 35 kDa, as deduced from its comparison with G $\beta_1$  (~37 kDa) and phosducin (~33 kDa; see Figs. 3 and 4). In summary, in *Xenopus* oocytes, m-c $\beta$ ARK is synthesized, myristoylated, and preferentially targeted to the membranes, as expected.

Next, we examined the effects of m-c $\beta$ ARK and additional G $\beta$  scavengers based on c- $\beta$ ARK on GIRK channels composed of subunits GIRK1 and GIRK2 (GIRK1/2). Oocytes were injected with either 0.2 ng/oocyte of RNA of each channel subunit (low/intermediate density of GIRK) or 1 ng/oocyte (high density of GIRK) (20) and 0.5 ng of RNA of the muscarinic m2 receptor, m2R. Fig. 2*A* shows typical recordings of K<sup>+</sup> currents without the coexpression of m-c $\beta$ ARK ("control") or with m-c $\beta$ ARK (5 ng of RNA/oocyte). In these whole-cell records,  $A_{\text{GIRK, basal}}$  is mirrored in the basal GIRK current,  $I_{\text{basal}}$  (*i.e.* the inward current that develops when the high Na<sup>+</sup> extracellular solution ND96 (96 mM Na<sup>+</sup>, 2 mM K<sup>+</sup>) is exchanged to a high K<sup>+</sup> solution (hK) with either 96 mM K<sup>+</sup> (Fig. 2*A*) or 24 mM K<sup>+</sup> (not shown). The agonist (acetylcholine; ACh)-induced current,  $I_{\text{ACh}}$ , was evoked by 10  $\mu$ M ACh. The total GIRK current,  $I_{\text{total}}$ , is  $I_{\text{basal}} + I_{\text{ACh}}$ . Oocytes that expressed c $\beta$ ARK showed greatly reduced  $I_{\text{basal}}$  and  $I_{\text{ACh}}$ . The inhibitory effect of m-c $\beta$ ARK was qualitatively and quantitatively similar in both 96 and 24 mM K<sup>+</sup> solutions (data not shown).

We examined the dose dependence of the effect of m-c $\beta$ ARK, titrating its expression level by injecting various amounts of RNA (RNA of GIRK subunits was 0.2 ng/oocyte in these experiments). As shown in Fig. 2*B*, the effect of m-c $\beta$ ARK on  $I_{\text{basal}}$  was dose-dependent and did not fully saturate at the highest dose of RNA used, 10 ng/oocyte. In contrast,  $I_{\text{ACh}}$  was completely inhibited at 5 ng of RNA/oocyte of m-c $\beta$ ARK. The data were fitted to a Michaelis-Menten-like equation, assuming that, at saturating doses, m-c $\beta$ ARK would fully block the GIRK currents. The fit yielded values of ED<sub>50</sub> (effective doses of RNA that cause 50% inhibition) of 3.04 and 0.1 ng of RNA/oocyte for  $I_{\text{basal}}$  and  $I_{\text{ACh}}$ , respectively. The estimate of ED<sub>50</sub> for  $I_{\text{ACh}}$  was intrinsically less accurate than for  $I_{\text{basal}}$ , due to very strong inhibition of  $I_{\text{ACh}}$  observed already at 2 ng of RNA/oocyte. Nevertheless, it reflects a much higher sensitivity of the evoked current to m-c $\beta$ ARK than of the basal one. Unfortunately, at 10 ng/oocyte, the expressed m-c $\beta$ ARK appeared to be toxic to oocytes, which often did not survive the 3–4-day incubation period. Therefore, in the following experiments, 5 ng/oocyte of m-c $\beta$ ARK RNA were routinely injected into the oocytes. We note that, in our hands, 5 or 10 ng of RNA/oocyte usually yielded very high levels of expressed proteins, because RNAs used in this study were designed to give maximal protein yield upon expression in the oocytes (see "Experimental Procedures").

To make sure that the decrease in GIRK currents by m-c $\beta$ ARK is not linked to changes in channel expression, we monitored the relative amounts of expressed GIRK channels in the PM using a confocal microscope-assisted immunocytochemistry method (Fig. 2*C*). The channels were visualized in very large plasma membrane patches (usually several thousand  $\mu\text{m}^2$ ), adhered to a coverslip, with their cytoplasmic surface facing the external medium (37). The patches were extensively washed and nominally free from endoplasmic reticulum.<sup>3</sup> As summarized in Fig. 2*C*, *b*, coexpression of m-c $\beta$ ARK did not affect the amount of channel protein in the PM.

Myristoylated m-c $\beta$ ARK seems to be suitable for the purpose of studying the G $\beta$  dependence of  $A_{\text{GIRK, basal}}$ , since it

<sup>3</sup> N. Dascal and E. Artzy, unpublished observations.

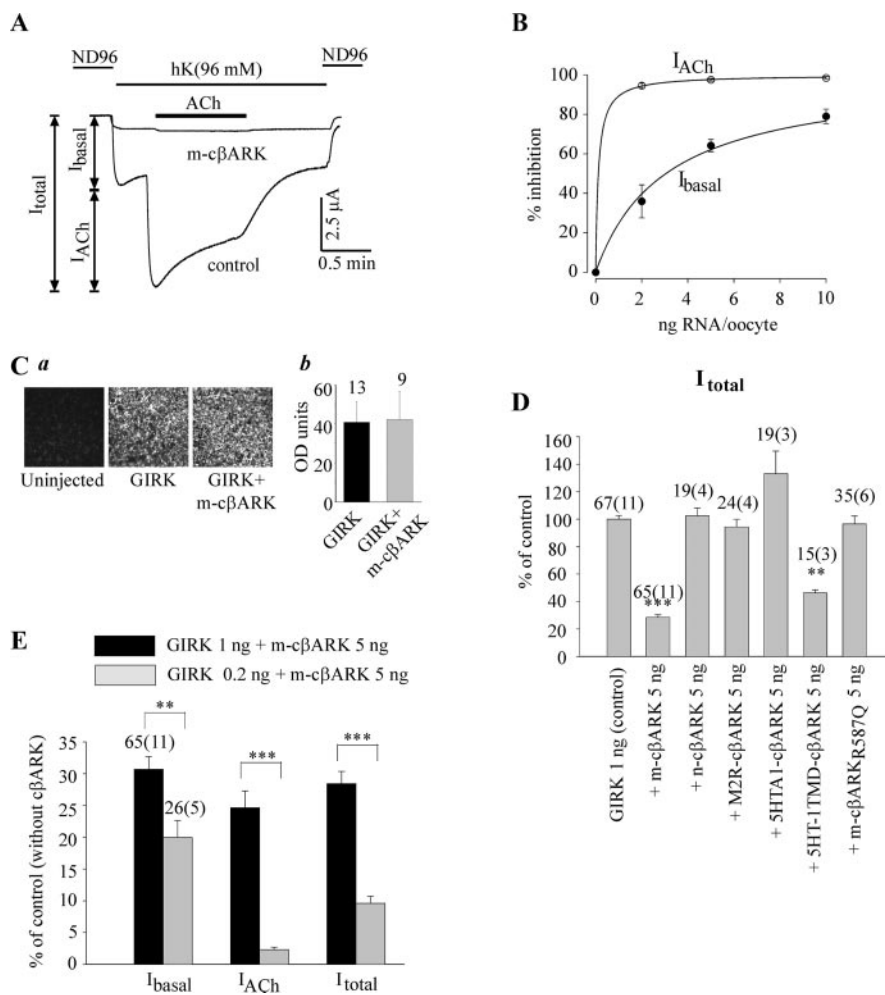


**FIG. 2. Effects of  $\beta$ ARK congeners on GIRK current.** *A*, examples of whole-cell GIRK currents measured by the two-electrode voltage clamp method. Oocytes were injected with 0.2 ng of RNA of each channel subunit and 0.5 ng of RNA of m2R with or without 5 ng of RNA of m-c $\beta$ ARK. *B*, extent of inhibition of  $I_{basal}$  and  $I_{ACh}$  is a dose-dependent function of the amount of injected RNA of m-c $\beta$ ARK. The solid lines show fits to the standard Michaelis-Menten equation for  $I_{basal}$ . *C*, coexpression of m-c $\beta$ ARK does not affect the level of expressed GIRK in the PM. *a*, representative confocal images of channel protein staining in large membrane patches. *b*, summary of the measurements of GIRK protein expression in the plasma membrane in oocytes of two donors. The net signal, in OD units, in each image was calculated by subtracting the average intensity of signal measured in uninjected oocytes. *D*, summary of effects of coexpression of different constructs containing  $\beta$ ARK on GIRK channel. The values of  $I_{total}$  are shown; changes in  $I_{basal}$  were similar. All parameters are shown as percentages of the same parameter recorded in the control group in the same experiment. *E*, the effect of coexpression of m-c $\beta$ ARK at high and low densities of the GIRK channel. Oocytes were injected with either 0.2 or 1 ng of RNA of each channel subunit and 0.5 ng of RNA of m2R, together or without 5 ng of RNA of m-c $\beta$ ARK. In *D* and *E*, the numbers above the bars denote the number of oocytes, with the number of experiments (oocyte batches) given in parentheses. Here and in the following figures, the statistical significance is denoted as follows: \*\* $p < 0.01$ ; \*\*\* $p \leq 0.001$ . The brackets below the asterisks show groups subjected to pairwise comparisons. The asterisks above the bars not denoted by brackets indicate statistically significant differences compared with the control group only.

does not block the direct Na<sup>+</sup>-induced activation (19). However, "side effects" are possible. One potential pitfall is that the G $\beta$ -binding segment is within a pleckstrin homology domain, which also binds PIP<sub>2</sub> (38); thus, heavily overexpressed  $\beta$ ARK may in principle reduce the amount of PIP<sub>2</sub> in the PM. Second, it is not known whether the myristoyl moiety affects the function of GIRK. To control for these possibilities, we constructed several membrane-targeted G $\beta$  scavengers based on c- $\beta$ ARK. First, we made a point mutation, R587Q, in m-c $\beta$ ARK, which greatly impairs the ability of c $\beta$ ARK to bind G $\beta$ , but not PIP<sub>2</sub> (39). Expression of this construct in the oocytes did not have any significant effect on GIRK currents (Fig. 2D), suggesting that PIP<sub>2</sub> chelation is not involved in the effect of m-c $\beta$ ARK. To check for possible "side effects" of the myristoyl moiety, we expressed the nonmyristoylated n-c $\beta$ ARK and found that it did not significantly affect GIRK currents at 5 ng of RNA/oocyte (Fig. 2D). Although n-c $\beta$ ARK (aa 460–689 of c $\beta$ ARK) is 8 aa shorter than m-c $\beta$ ARK (aa 452–689), both constructs contain the G $\beta$ -binding domain

(aa 643–670) as well as the full pleckstrin homology domain (aa 561–655) (39). Therefore, the difference in length probably does not determine the difference in the effect on GIRK currents. Next, we constructed fusion proteins in which c- $\beta$ ARK was connected to C-terminal ends of several membrane proteins, which were expected to anchor these tandems to the PM, instead of the myristoyl moiety. The proteins chosen were m2R, the serotonin receptor 5HT1AR, and the first transmembrane domain of 5HT1AR, 5HT-1TMD. The first two constructs did not inhibit GIRK currents (Fig. 2D) after 3 days of incubation. Mild inhibitory effects of m2R-c $\beta$ ARK and 5HT1A-c $\beta$ ARK were seen after long periods of oocyte incubation, 4–5 days (data not shown), suggesting that these very large fusion proteins may be poorly expressed in the oocytes. However, 5HT-1TMD-c $\beta$ ARK significantly reduced  $I_{total}$  though less than m-c $\beta$ ARK (by ~55%, versus ~72% inhibition by c $\beta$ ARK; Fig. 2D). This result suggests that the presence of the myristoyl moiety is not necessary for c- $\beta$ ARK to inhibit GIRK.

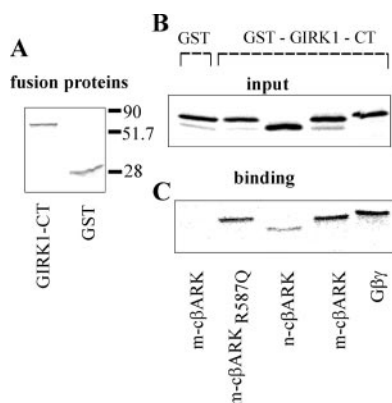


FIG. 3. **c $\beta$ ARK binds to C terminus of GIRK1.** Binding of different c $\beta$ ARK congeners to the GST-fused C terminus of GIRK1 (GST-GIRK1-CT) is shown in comparison with G $\beta$  $\gamma$  synthesized *in vitro* in rabbit reticulocyte lysate. Representative of two experiments. **A**, Coomassie Blue staining of GST (used as control) and GST-GIRK1-CT. **B** and **C**, Phosphor-Imager autoradiogram of *input* (**B**) (i.e. the radioactive signal from a 5- $\mu$ l sample taken of the 300- $\mu$ l reaction mixture before the addition of glutathione affinity beads) and *binding* (**C**) of the proteins to the GST fusion protein (the bound protein eluted from the beads with glutathione).

Next, we compared the effect of m-c $\beta$ ARK on GIRK channels expressed at two different densities. Coexpression of m-c $\beta$ ARK (5 ng RNA/oocyte) was less effective in reducing  $I_{\text{basal}}$  and  $I_{\text{ACh}}$  when more channels were expressed (Fig. 2*E*). At high channel density (1 ng RNA/oocyte),  $I_{\text{basal}}$  was decreased by  $\sim 70\%$ , and  $I_{\text{ACh}}$  was decreased by  $\sim 75\%$ , in comparison with  $\sim 80$  and  $\sim 95\%$  decrease, respectively, at lower channel density, 0.2 ng of RNA/oocyte. The same held true for  $I_{\text{total}}$ . These differences are not unexpected for a pure G $\beta$  $\gamma$  scavenger whose efficiency depends on the ratio of its own concentration to that of the G $\beta$  $\gamma$ -binding effector (GIRK) under study, as well as on the cellular level of G $\beta$  $\gamma$  (see Fig. 8). Another possibility is that the scavenger interacts with the effector (GIRK in our case) and is itself sequestered by high doses of the channel, so that the efficiency of G $\beta$  $\gamma$  sequestration is reduced. Indeed, GIRK and  $\beta$ ARK co-immunoprecipitate, along with a number of other components of a multiprotein signaling complex, from atrial cells (40).

The possibility of a direct interaction between c $\beta$ ARK and GIRK was probed using the standard pull-down methodology. We used a purified GST fusion protein containing the full-length cytosolic C terminus of GIRK1, GST-GIRK1-CT (aa 183–501), which was previously shown to bind G $\beta$  $\gamma$  (21, 27, 41). Unexpectedly, we found that GST-GIRK1-CT bound [ $^{35}$ S]methionine-labeled m-c $\beta$ ARK and m-c $\beta$ ARK<sub>R587Q</sub> synthesized *in vitro* in reticulocyte lysate almost as well as it bound G $\beta$  $\gamma$  (Figs. 3 and 4*B*). n-c $\beta$ ARK also bound to GST-GIRK1-CT, but distinctly more weakly than m-c $\beta$ ARK. At present, we do not know whether this difference was due to the absence of myristoylation or of the first 8 aa in n-c $\beta$ ARK. Because m-c $\beta$ ARK<sub>R587Q</sub>, which binds GIRK1 but not G $\beta$  $\gamma$ , does not affect GIRK currents (Fig. 2), it is plausible that most of the inhibitory effect of m-c $\beta$ ARK is independent of its binding to GIRK and represents a genuine G $\beta$  $\gamma$  scavenging effect. However, the direct interaction between m-c $\beta$ ARK and GIRK1 is bound to complicate the interpretation of the results of this and previous studies.

**A Novel G $\beta$  $\gamma$  Scavenger, m-phosducin, Reveals That Most  $A_{\text{GIRK,basal}}$  Is G $\beta$  $\gamma$ -dependent at All Channel Densities**—In a search for a G $\beta$  $\gamma$  scavenger that does not interact with GIRK, we constructed a myristoylated first intracellular loop of the N-type voltage-dependent Ca $^{2+}$  channel, which is known to bind G $\beta$  $\gamma$  (42). However, expression of this construct in the oocytes led to a rather weak inhibition of GIRK currents (data

not shown). Next, we turned to phosducin, a soluble cytosolic G $\beta$  $\gamma$ -binding protein originally identified in retinal photoreceptor cells, which has already been used as a G $\beta$  $\gamma$  scavenger in heterologous expression systems (43). Phosducin also binds G $\alpha$ , but this interaction is of much lower affinity than that with G $\beta$  $\gamma$  (44). In this paper, we designate the original cytosolic phosducin as n-phosducin to distinguish it from the myristoylated construct made by us.

Coexpression of n-phosducin (10 ng of RNA/oocyte) reduced  $I_{\text{basal}}$  by  $\sim 70\%$  and  $I_{\text{ACh}}$  by only  $\sim 42\%$  (see Fig. 5*B*). To increase the likelihood that phosducin will access G $\beta$  $\gamma$  in the PM, we constructed a DNA for myristoylated m-phosducin. The resulting protein has an added 15-aa myristoylation signal, the same as in m-c $\beta$ ARK, at the beginning of its N terminus. n-Phosducin expressed in the oocytes was preferentially associated with the cytosolic fraction, whereas m-phosducin was enriched in the membrane fraction (Fig. 4*A*). Pull-down experiments showed that neither n-phosducin nor m-phosducin bound GST-GIRK1-CT (Fig. 4*B*). Since the N terminus of GIRK1 also binds G $\beta$  $\gamma$  (27), we examined whether the GST-fused N terminus of GIRK1 (GST-GIRK1-NT) binds c $\beta$ ARK and phosducin. Fig. 4*D* shows that GST-GIRK1-NT bound G $\beta$  $\gamma$  and, to a lesser extent, m-c $\beta$ ARK, but neither n-phosducin nor m-phosducin interacted with the N terminus of GIRK1. Coexpression of m-phosducin did not affect the amount of expressed GIRK channels in the PM of *Xenopus* oocytes (Fig. 4*D*). Thus, m-phosducin has the desired properties of a PM-enriched G $\beta$  $\gamma$  scavenger that does not interact with GIRK.

Coexpression of m-phosducin with GIRK at 10 ng RNA/oocyte efficiently decreased GIRK currents (Fig. 5*A*). The effect of phosducin was dose-dependent (see below) and did not saturate at the maximal RNA dose used, 10 ng/oocyte (this dose was not toxic and was routinely used in all experiments, unless stated otherwise). We compared the effects of m-phosducin (10 ng of RNA/oocyte) on GIRK currents at low/intermediate (0.2 ng/oocyte) and high (1 ng of RNA/oocyte) channel densities (Fig. 5, *B* and *C*). m-Phosducin reduced  $I_{\text{basal}}$  to about the same extent, by 85–90%, at both channel densities. However, it was less effective than m-c $\beta$ ARK in reducing peak  $I_{\text{ACh}}$  in comparison with m-c $\beta$ ARK. The inhibition of  $I_{\text{ACh}}$  by m-phosducin was stronger at lower channel densities, suggesting competition among G $\alpha$ , GIRK, and m-phosducin for available G $\beta$  $\gamma$ . n-Phosducin was significantly less effective than m-phosducin in reducing GIRK currents. To examine whether the 10–15%  $I_{\text{basal}}$  remaining in the presence of m-phosducin are G $\beta$  $\gamma$ -dependent, we coexpressed, in addition, m-c $\beta$ ARK (5 ng/oocyte). This treatment did not further reduce  $I_{\text{basal}}$ , supporting the possibility of the presence of measurable G $\beta$  $\gamma$ -independent basal activity in GIRK channels (Fig. 5*B*). However, the main outcome of these experiments is that up to 90% of  $A_{\text{GIRK,basal}}$  is G $\beta$  $\gamma$ -dependent.

$I_{\text{ACh}}$  of GIRK channels expressed in *Xenopus* oocytes slowly decays in the continuous presence of ACh, reaching a steady state after 3–5 min (45, 46). We noticed that, in the presence of m-phosducin, the decay was strongly accelerated. The steady state level of  $I_{\text{ACh}}$  was greatly diminished compared with control (see Fig. 5*A*). The kinetics of decay of  $I_{\text{ACh}}$  were specifically studied in a separate experiment ( $n = 6$  oocytes). Fig. 6*A* shows representative records from two oocytes, with and without coexpressed m-phosducin, after scaling the peak  $I_{\text{ACh}}$  currents to facilitate the comparison of decay kinetics. Fig. 6*B* summarizes the effects of m-phosducin on the amplitudes of  $I_{\text{basal}}$  and  $I_{\text{ACh}}$  measured at the peak and 1.5 min after the addition of ACh. On the average, within 1.5 min,  $I_{\text{ACh}}$  decayed to a mere  $2.7 \pm 1.3\%$  of  $I_{\text{ACh}}$  measured at the same time point in control oocytes. The time constant of decay of  $I_{\text{ACh}}$  in the continuous presence of ACh,  $\tau_{\text{decay}}$ , decreased from 34 s in control to less than 5 s in the

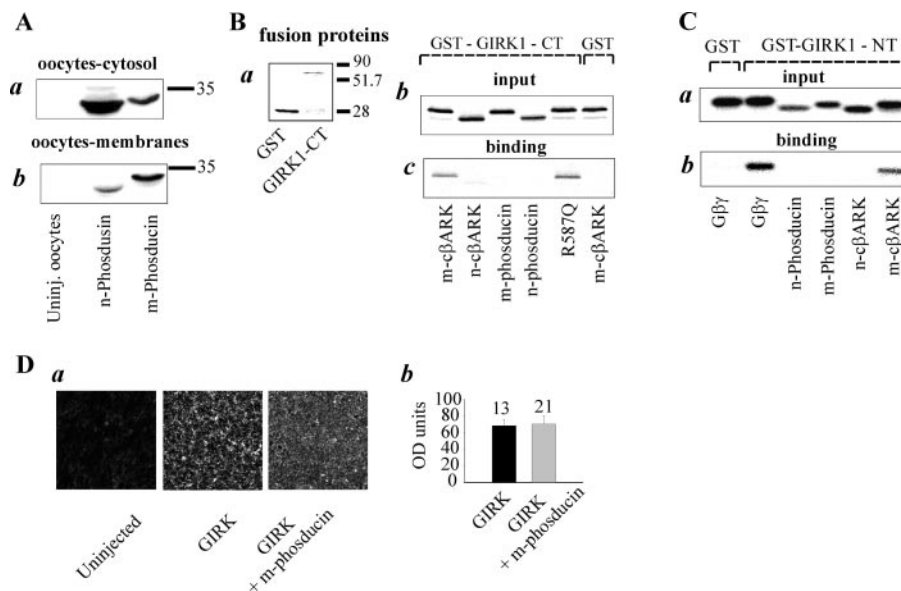


**FIG. 4. Characterization of the properties of n-phosducin and m-phosducin.** *A*, myristoylation promotes the association of m-phosducin with membranes. Oocytes expressing phosducin were separated into cytosol and membrane fractions by differential centrifugation, and phosducin protein was visualized using Western blot. Both n-phosducin and m-phosducin were present in the cytosol (*a*), but m-phosducin was enriched in the membrane fraction (*b*) compared with n-phosducin. *B*, test of binding of phosducin to GST-GIRK1-CT, in comparison with different c $\beta$ ARK congeners (two experiments). c- $\beta$ ARK and phosducin derivatives were synthesized *in vitro* in rabbit reticulocyte lysate. The *left panel (a)* shows Coomassie Blue staining of GST-GIRK1-CT and GST. The *right panels* show PhosphorImager autoradiograms of *input (b)* and *binding of in vitro* synthesized proteins to GST-GIRK1-CT or GST (*c*). For explanation of the terms *input* and *binding*, see the legend to Fig. 3. *C*, test of binding of phosducin to GST-GIRK1-NT, in comparison with c $\beta$ ARK and G $\beta$  $\gamma$ . PhosphorImager autoradiogram of *input (a)* and *binding (b)* of *in vitro* synthesized proteins to GST-GIRK1-NT or GST are shown. *D*, m-phosducin does not affect the expression of GIRK in the PM. *a*, representative confocal images of channel protein staining in large membrane patches of oocytes. *b*, summary of the measurements of GIRK protein expression (1 ng RNA/oocyte) in the PM, after subtraction of the average intensity of signal measured in uninjected oocytes, in three separate experiments (oocyte batches).

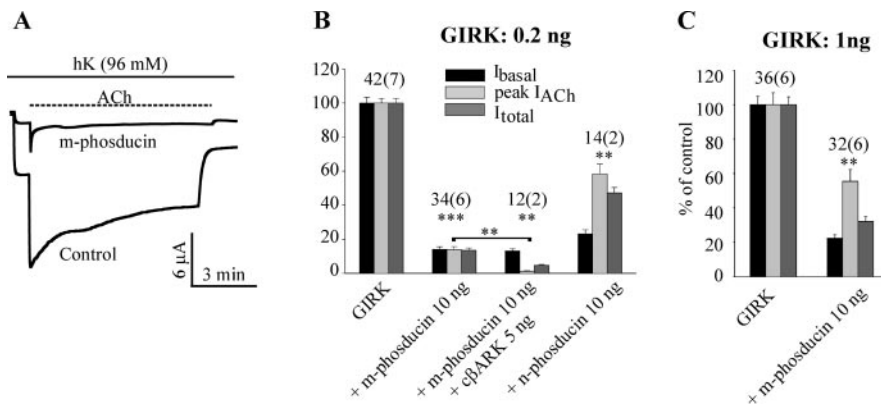


**FIG. 5. G $\beta$  $\gamma$  scavengers cannot completely inhibit the basal activity of GIRK.** *A*, representative current records in oocytes expressing the channel alone or with m-phosducin. Oocytes were injected with 0.2 ng of RNA of each channel subunit and 0.5 ng of RNA of m2R with or without 10 ng RNA of m-phosducin. *B*, summary of effects of coexpression of m-phosducin, n-phosducin, and m-phosducin together with m-c $\beta$ ARK, at low/intermediate density of the GIRK channel. All parameters are shown as percentage of the same parameter recorded in the control group. Note that coexpression of c $\beta$ ARK on top of m-phosducin further reduces  $I_{ACh}$  ( $p < 0.01$ ) but does not further reduce  $I_{basal}$ . *C*, summary of the effect of coexpression of m-phosducin at high density of the GIRK channel.

presence of m-phosducin; thus, in the latter case, by 1.5 min a steady state was reached (Fig. 6C). No change in speed of activation could be detected, but the speed limit of the perfusion system used ( $\sim 1$  s) did not enable a conclusive measurement. The effect of phosducin is readily understood in general kinetic terms and can be quantitatively described by a kinetic model (not shown), assuming a simple competition among GIRK, G $\alpha_{GDP}$ , and m-phosducin for available G $\beta$  $\gamma$ , as follows. The extent of inhibition of  $I_{basal}$  is determined by the concentrations of the proteins involved and by the actual  $K_D$  values, since the system has sufficient time to reach equilibrium. At equilibrium, a certain percentage of G $\beta$  $\gamma$  is bound to G $\alpha$  within heterotrimers and is liberated from G $\alpha$  upon activation by agonist. This leads to an initial increase in free G $\beta$  $\gamma$  concentration, followed by re-equilibration and capturing of much of the G $\beta$  $\gamma$  by the scavenger. The

initial large peak of  $I_{ACh}$  can be explained kinetically by assuming that G $\beta$  $\gamma$  released upon transmitter activation first gets access to the channel and only later can be captured by the scavenger. This supports the view that a G $\alpha$ G $\beta$  $\gamma$  complex is closely associated with GIRK (see "Discussion"), although a similar property can also be conferred by a kinetic characteristic (a "slow" scavenger with a low on-rate).

Measurements of the kinetics of  $I_{ACh}$  in the presence of coexpressed m-c $\beta$ ARK have been attempted but proved less reliable, since m-c $\beta$ ARK reduced peak  $I_{ACh}$  more potently than m-phosducin. However, in those oocytes where  $I_{ACh}$  could be reliably measured in the presence of m-c $\beta$ ARK,  $I_{ACh}$  did not show any fast decay (Fig. 6D; representative of at least 20 cells).

The dependence of the effect of m-phosducin on level of its

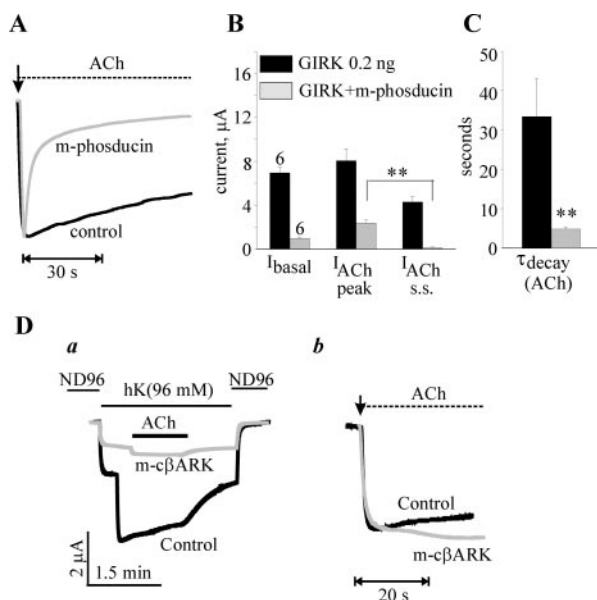


**FIG. 6. Kinetic aspects of the effect of m-phosducin on  $I_{\text{ACh}}$ .** *A*, comparison of kinetics of inactivation of  $I_{\text{ACh}}$ , in the same oocytes shown in Fig. 5*A*.  $I_{\text{ACh}}$  in the m-phosducin-expressing oocyte was scaled to  $I_{\text{ACh}}$  in the control oocyte to illustrate the differences in current kinetics. *B*, summary of amplitudes of  $I_{\text{ACh}}$  at the peak and in steady state (measured 1.5 min after the peak) in six oocytes of the same batch. *C*, m-phosducin accelerates the inactivation of  $I_{\text{ACh}}$ . *D*, c- $\beta$ ARK (5 ng of RNA/oocyte) does not accelerate the inactivation of  $I_{\text{ACh}}$ . GIRK was expressed at 1 ng of RNA/oocyte. Original current records (*a*) were scaled up (*b*) to illustrate the differences in current kinetics.

expression was studied in two separate experiments. The results are shown in Fig. 7, where they are compared with the dose dependence of m-c $\beta$ ARK from Fig. 2 (*gray lines*). m-phosducin reduced  $I_{\text{basal}}$  similarly to m-c $\beta$ ARK, with an  $\text{ED}_{50}$  of 2.1 ng of RNA/oocyte. Remarkably, the effect of m-phosducin on  $I_{\text{ACh}}$  was strikingly different from that of c $\beta$ ARK. The dose dependence of inhibition of peak  $I_{\text{ACh}}$  (*open circles*) was very similar to that for  $I_{\text{basal}}$  (*closed circles*), practically falling on the same Michaelis-Menten curve. Because  $\text{ED}_{50}$  is conceptually similar to dissociation constant,  $K_D$ , which is a measure of the equilibrium state, we have also measured the dose dependence of inhibition of steady state  $I_{\text{ACh}}$  (Fig. 7, *triangles*). Again, it was very similar to that of  $I_{\text{basal}}$  and peak  $I_{\text{ACh}}$ .

**Expression of GIRK Is Accompanied by an Increase in the Amount of G $\beta$  $\gamma$  in the PM**—We have previously shown that the amount of endogenous G $\beta$  $\gamma$  measured by Western blot methodology in total cellular membrane fraction of *Xenopus* oocytes does not change appreciably when GIRK is overexpressed (20). How can  $A_{\text{GIRK,basal}}$  remain 90% G $\beta$  $\gamma$ -dependent when more and more channels are expressed if free G $\beta$  $\gamma$  concentration stays constant and there is less and less G $\beta$  $\gamma$  per channel? One possibility is that the expression of GIRK leads to an increase in the amount of G $\beta$  $\gamma$  in the PM. To explore this possibility, we monitored changes in GIRK1/2, G $\beta$  $\gamma$ , and G $\alpha$  in large patches of PM, using the imaging method described above (see Fig. 2*C*). The proteins were visualized by a GIRK1 antibody, a common G $\beta$  antibody that recognizes G $\beta$  subunits 1–4 but not G $\beta_5$ , and a common G $\alpha$  antibody that recognizes all G $\alpha$  subunits. Fig. 8 demonstrates that the increase in the amount of GIRK in the membrane, brought about by injection of RNA, was accompanied by an increase in the amounts of endogenous G $\alpha$  and G $\beta$  in the PM. Specificity of labeling was controlled for by incubating the PM patches with the antibodies in the presence of an excess of the respective antigens (purified G $\alpha_{11}$  or G $\beta_{1\gamma_2}$ ). With both G $\alpha$  and G $\beta$  $\gamma$ , the background labeling remaining in the presence of the antigen was the same in native and GIRK-

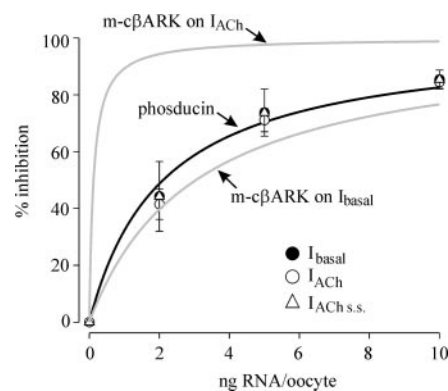


**FIG. 7. Dose dependence of m-phosducin inhibition of  $I_{\text{basal}}$  and  $I_{\text{ACh}}$ : A comparison with m-c $\beta$ ARK.** Oocytes were injected with 0.2 ng of RNA of each channel subunits, 0.5 ng of RNA of m2R, and different amounts of RNA of m-phosducin. Results from two batches of oocytes are summarized; each point represents mean  $\pm$  S.E. of 6–9 cells. The *solid black line* is a fit to the standard Michaelis-Menten equation for  $I_{\text{basal}}$ ; the *fitted lines* for  $I_{\text{ACh}}$  (peak and steady state) were very similar. The *gray lines* show the dose response for m-c $\beta$ ARK from Fig. 2*B*.

expressing oocytes, suggesting a complete block of the specific labeling by both antigens. In uninjected (native) oocytes, the endogenous G $\alpha$  label was clearly above the background (Fig. 8*A*), whereas the endogenous G $\beta$  $\gamma$  could not be clearly detected in this experiment (Fig. 8*B*). In the presence of coexpressed GIRK (2.5 ng of RNA/oocyte), both G $\beta$  and G $\alpha$  rose significantly above the control level. After subtraction of the background fluorescence, net increase in G $\beta$  label was from an undetectable level to  $\sim 25$  OD units ( $p < 0.001$ ), whereas the level of G $\alpha$  increased from  $\sim 25$  to  $\sim 38$  OD units ( $p < 0.05$ ) (*i.e.* less than 2-fold). Although this rough comparison does not provide true quantification of the increase in G $\alpha$  versus G $\beta$  levels, it appears to indicate that the relative increase in the level of G $\beta$ , caused by the expression of GIRK, was greater than that of G $\alpha$ .

Fig. 8*C* shows that the expression of the GIRK protein in the PM increased with an increase in the dose of injected RNA. The background labeling with the GIRK1 antibody in uninjected oocytes was very low, suggesting high specificity of the antibody and the expected absence of GIRK1 protein in native oocytes. Fig. 8*D* summarizes a separate series of experiments in which the levels of G $\alpha$  and G $\beta$  in the PM were measured upon the expression of GIRK at two different levels. The levels of both G protein subunits were increased already when a low dose of GIRK RNA, 0.1 ng/oocyte, was injected, and a further increase was observed upon injection of a high dose of GIRK RNA, 2.5 ng.

## DISCUSSION

**Most of the Basal Activity of GIRK Is G $\beta$  $\gamma$ -dependent at All Levels of GIRK Expression**—Basal activity of GIRK channels,  $A_{\text{GIRK,basal}}$ , is observed in the absence of agonist and, in heterologous expression systems, of any coexpressed receptor (2). To understand the mechanisms underlying  $A_{\text{GIRK,basal}}$ , we utilized *Xenopus* oocytes, unsurpassed for titrated expression of proteins for rigorous quantitative studies (which we term “expression pharmacology”). Of the several G $\beta$  $\gamma$  scavenger constructs used here, myristoylated derivatives of c $\beta$ ARK and phosducin proved most efficient. The two scavengers have similar high affinities of binding to G $\beta$  $\gamma$  *in vitro*:  $K_D$  of 42 nM in a detergent solution for phosducin (47) and 32 nM in phospholipid vesicles for  $\beta$ ARK (48). Myristoylation ensured preferential incorporation of these proteins into membrane fractions and, in parallel, stronger inhibition of GIRK activity than by nonmyristoylated congeners. The strong reduction of GIRK currents by c $\beta$ ARK fused to the first transmembrane domain of the 5HT $_1A$  recep-

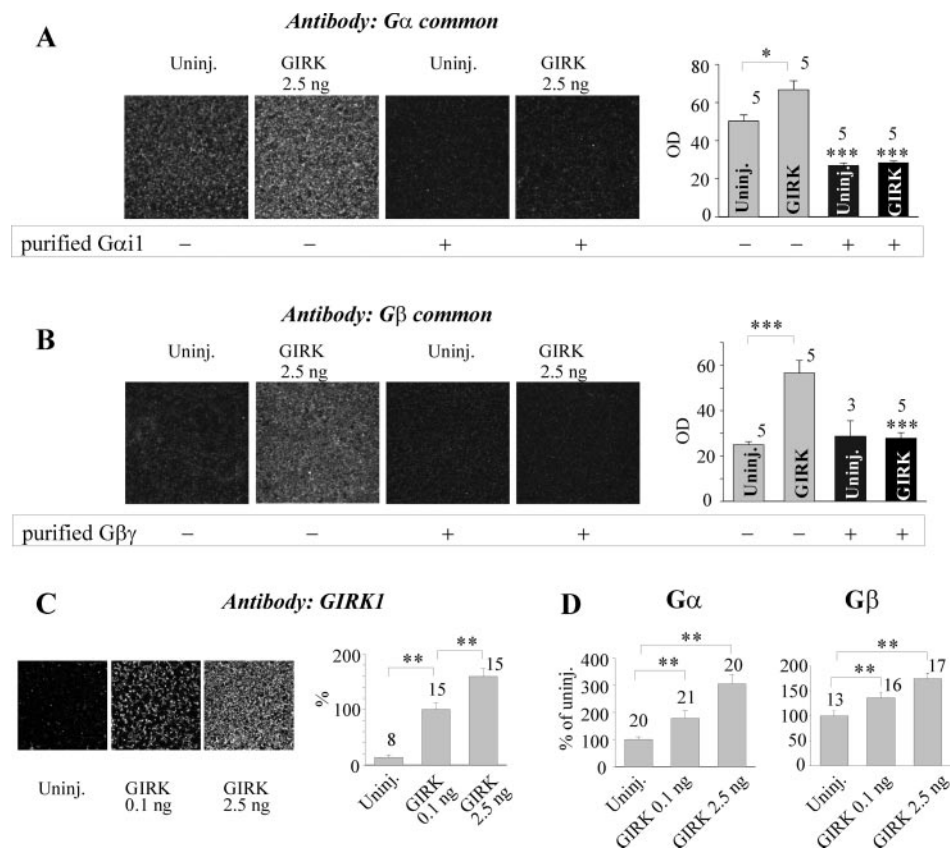


**FIG. 8. Expression of GIRK is accompanied by an increase in the amount of endogenous G $\alpha$  and G $\beta$  in the plasma membrane.** In *A* and *B*, the levels of G $\alpha$  (*A*) and G $\beta$  (*B*) were measured by immunocytochemistry in large PM patches. The *left panels* show representative confocal microscope images of the membrane patches labeled with the respective antibodies. The *right panels* summarize the label intensities measured in patches from oocytes of the same donor frog (numbers of patches imaged are shown above the bars). The labeling remaining in the presence of excess antigens (*black bars*; G $\alpha$ <sub>i1</sub>-GDP in *A* and G $\beta$ <sub>1 $\gamma$ 2</sub> in *B*) represents nonspecific background fluorescence. The levels of nonspecific signal were compared with total signal observed in the absence of the antigen (*asterisks above black bars*) separately for native and for GIRK-expressing oocytes. *C*, the level of expressed GIRK1 in PM patches increases as a function of the amount of injected RNA. The *right panel* summarizes data from three oocyte batches. Nonspecific labeling in the absence of expressed channel was very low; therefore, the level of GIRK1 was normalized to that observed in oocytes injected with 0.1 ng of RNA. *D*, summary of data from two or three oocyte batches showing the increase in the level of endogenous G $\alpha$  and G $\beta$  upon coexpression of GIRK1/2 at two RNA doses, 0.1 and 2.5 ng/oocyte. Data were normalized to control levels of G $\beta$  or G $\alpha$  detected in uninjected (*Uninj.*) oocytes. In these experiments, nonspecific labeling was not estimated, and the measured values represent total fluorescence signal (background + specific).

tor suggests that the myristoyl moiety itself is not essential; rather, membrane anchoring appears to be the important factor that ensures efficient competition between a G $\beta$  $\gamma$  scavenger and GIRK for membrane-attached G $\beta$  $\gamma$ . Unfortunately, we find that, in addition to sequestering G $\beta$  $\gamma$ , m-c $\beta$ ARK directly binds to GIRK1. This interaction does not seem to interfere with the activation of the channel by G $\beta$  $\gamma$ , because m-c $\beta$ ARK<sub>R587Q</sub>, which does not bind G $\beta$  $\gamma$  but still binds GIRK1, has no effect on GIRK currents. Despite this consideration, the binding of m-c $\beta$ ARK to GIRK1 is a serious disadvantage that perplexes the interpretation of the experimental results.

Both m-phosducin and m-c $\beta$ ARK reduced  $I_{\text{basal}}$  in a dose-dependent manner. RNA titration experiments showed a slightly lower ED<sub>50</sub> for m-phosducin, possibly due to better protein expression or PM accumulation of m-phosducin. Titrated expression of these two potent G $\beta$  $\gamma$  scavengers, performed in a rigorous quantitative manner for the first time here, led us to the main empirical conclusion of this work; at least 90% of  $A_{\text{GIRK,basal}}$  in intact oocytes is G $\beta$  $\gamma$ -dependent at all densities of GIRK channels.

The source of G $\beta$  $\gamma$  that determines  $A_{\text{GIRK,basal}}$  in the oocytes and other cells is not clear. It is widely believed that the G $\beta$  $\gamma$ -dependent component of  $A_{\text{GIRK,basal}}$  reflects the concentration of free G $\beta$  $\gamma$  in the membrane (2). The most obvious and best studied sources of free G $\beta$  $\gamma$  in the PM are the G $\alpha$  $\beta$

heterotrimers. The latter dissociate and supply free G $\beta$  $\gamma$  by several mechanisms: basal dissociation of G $\alpha_{\text{GDP}}$  from G $\beta$  $\gamma$  in the absence of GDP-GTP exchange (49); basal GDP-GTP exchange that results in great reduction of the affinity of G $\alpha$  to G $\beta$  $\gamma$  (50); and GPCR-catalyzed GDP-GTP exchange that occurs as a result of a constitutive activity of the GPCR in the absence of an agonist (51) or is induced by an ambient agonist present in the extracellular medium (the latter seems unlikely in isolated, follicle-free, constantly perfused oocyte preparations). Estimation of the relative contribution of these processes to  $A_{\text{GIRK,basal}}$  in oocytes and other cells will require further study.

**GIRK May Be Constitutively Associated with G $\beta$  $\gamma$** —The idea that many end effectors of GPCRs operate within multiprotein complexes that include the GPCRs, heterotrimeric G proteins, and effectors themselves has gained wide acceptance (52). It has been proposed that, under normal physiological conditions, GIRK is associated with a G $\alpha_{\text{o}}$  $\beta$  $\gamma$  complex, which guarantees both low  $A_{\text{GIRK,basal}}$  and rapid and efficient channel activation by G $\beta$  $\gamma$  released upon an encounter with an agonist-bound GPCR (20, 26–28, 40, 53). The observation that the levels of endogenous G $\beta$  $\gamma$  and G $\alpha$  in PM increase upon expression of GIRK (Fig. 8) provides new support to this hypothesis and further extends it, indicating that GIRK is preassociated with G $\beta$  $\gamma$  and G $\alpha$  in the endoplasmic reticulum or the Golgi complex before being relocated to the PM. Joint trafficking of



ion channels and associated proteins is a well documented phenomenon (e.g. see Ref. 54). The change in Gβγ levels was not previously detected in total membrane fraction (20), probably because of the very low surface/volume ratio in the oocyte, where the PM constitutes at best a few percent of total cellular membranes.

The protein complex comprising GIRK and G protein subunits may also contain other components, such as protein kinase A, phosphatases, and βARK (40). It is probable that the complex is a dynamic one and that the interactions within it are reversible, as indicated by the ability of exogenously expressed Gα such as Gα<sub>s</sub> and Gα<sub>z</sub> to replace the endogenous Gα<sub>i/o</sub> (32, 55) and by the finite affinities of protein-protein interactions *in vitro*. On the other hand, there are indications that the complex may be rather stable: the components are co-precipitated by a single antibody (40); pull-down experiments show strong binding between GIRK and Gα, Gβγ, and βARK (see Refs. 21, 27, and 41 and Fig. 3); and known affinities of interactions among some of the protein components are in the nanomolar range (Gβγ-GIRK, <10 nM; Gα-Gβγ, 0.2–2 nM) (discussed in Ref. 56).

A stable association of GIRK with Gβγ, together with the increase in Gβγ levels in PM, provides the basis for an understanding of the excessively high  $A_{\text{GIRK,basal}}$  at high GIRK densities. Although the level of endogenous Gα also rises upon coexpression of GIRK, it appears insufficient to prevent the disproportional increase in  $A_{\text{GIRK,basal}}$ , possibly because the increase in the level of Gβγ in the PM is greater than that of Gα. Comparison of the relative increases in Gα and Gβ caused by the expression of GIRK (Fig. 8, A and B) seems to support this possibility. However, at present this interpretation remains presumptive, because the immunocytochemistry method used here, although sensitive, does not provide quantitative information on the absolute levels of proteins measured with different antibodies. It is also possible that the observed rise in Gα levels includes that of “irrelevant” Gα (not Gα<sub>i/o</sub>) available in the oocytes, which cannot efficiently reduce  $A_{\text{GIRK,basal}}$  and/or donate Gβγ upon activation of m2R.

In summary, our observations so far conform to the proposal (20, 28) that  $A_{\text{GIRK,basal}}$  is controlled by both Gβγ and Gα. Expression of GIRK is accompanied by a rise in ambient Gβγ available for activation of GIRK, which is not accompanied by a comparably strong rise in the level of Gα<sub>i/o</sub> subunits, thus causing an excessively high  $A_{\text{GIRK,basal}}$ . Taking together the previously accumulated evidence regarding the existence of GIRK-Gαβγ complexes and the new data presented here, we propose that GIRK is persistently, although reversibly, associated with Gα<sub>GDP</sub>βγ throughout its biosynthesis; Gα is a nonobligatory part of the complex, whereas Gβγ is bound persistently.

*Using m-phosducin and m-cβARK to Assess the Existence of Different Gβγ-binding Sites in GIRK*—It has been proposed, on the basis of mutational analysis of GIRK1 and GIRK4, that agonist-evoked activity is mediated by binding of Gβγ to a low affinity site(s), and  $A_{\text{GIRK,basal}}$  depends on the interaction of Gβγ with another, high affinity, site(s) in the GIRK protein (57). Later works suggested that an intact putative site underlying  $A_{\text{GIRK,basal}}$  is also crucial for agonist-evoked activity (58) and that a residue implicated in low affinity Gβγ binding (57) may be involved in channel gating rather than Gβγ binding (21, 59). Thus, the issue of two types of Gβγ-binding site remains unresolved.

Gβγ scavengers can be used to probe the existence in GIRK of Gβγ-binding sites with different affinities to Gβγ. The concentration of Gβγ required to induce  $A_{\text{GIRK,basal}}$  via the high affinity site of GIRK would be lower than that required to induce  $I_{\text{ACH}}$  via the low affinity site. Consequently, less Gβγ

scavenger would be needed to suppress activation of GIRK by Gβγ released following GPCR activation than by ambient Gβγ that determines  $A_{\text{GIRK,basal}}$ . Alas, the results with the two potent Gβγ scavengers used here were not unequivocal. m-phosducin and m-cβARK showed striking differences in the apparent potency of inhibition of peak  $I_{\text{ACH}}$  and in  $\text{ED}_{50}$ . The data obtained with cβARK appear to support the two-site model of He *et al.* (57);  $I_{\text{ACH}}$  was inhibited by much lower doses of m-cβARK than  $I_{\text{basal}}$ . However, m-phosducin, which showed an even greater apparent affinity in inhibiting  $A_{\text{GIRK,basal}}$  than m-cβARK (Fig. 7), exhibited an identical apparent affinity for  $I_{\text{ACH}}$ .

A clue for the understanding of these differences may be provided by invoking the fact that m-cβARK binds GIRK. Phosducin reduced  $I_{\text{basal}}$  stronger than  $I_{\text{ACH}}$  but accelerated the decay of  $I_{\text{ACH}}$ . These effects of m-phosducin are compatible with those of a simple Gβγ sink (see “Results”). In contrast, m-cβARK inhibited  $I_{\text{ACH}}$  with a high apparent affinity but did not accelerate its decay. It can be shown that such properties can be conferred by very fast Gβγ scavenging by cβARK, such that it captures Gβγ released from the heterotrimeric Gαβγ before Gβγ can reach the channel. Anchoring of c-βARK to the channel would enable such extra fast scavenging. More complicated schemes, which assume the formation of a high affinity triple cβARK-Gβγ-GIRK complex, or a competition between m-cβARK and Gβγ for binding to GIRK may also explain the effects of m-cβARK described here. Unfortunately, all interpretations are complicated by the fact that GIRK directly binds cβARK, and its use as a “straightforward” Gβγ scavenger in GIRK studies should be avoided.

To summarize, we contend that, as a Gβγ scavenger, m-cβARK is inferior to m-phosducin in GIRK studies. The results obtained with m-phosducin are consistent with the existence of a single type of Gβγ binding site underlying both basal and agonist-evoked activation of GIRK or the existence of separate sites with very similar affinities for Gβγ.

*Possible Mechanism of Gβγ-independent Basal Activity*—Inhibition of the whole-cell basal GIRK current,  $I_{\text{basal}}$ , by both scavengers used here was dose-dependent and did not fully saturate even at the highest dose of scavengers used. Therefore, we cannot state with certainty that the remaining ~10–15% of  $A_{\text{GIRK,basal}}$  is Gβγ-independent. The fact that the expression of c-βARK at 5 ng of RNA/oocyte (a dose that normally inhibits 70–80% of  $I_{\text{basal}}$ ) on top of phosducin did not further reduce  $I_{\text{basal}}$  supports the existence of a Gβγ-independent component. This putative Gβγ-independent component of  $A_{\text{GIRK,basal}}$ , although small, is not negligible and may be physiologically relevant. It is also interesting from the biophysical point of view. What determines the open-closed equilibrium of GIRK in the absence of the main physiological gating factor, Gβγ? “Spontaneous” transitions from closed to open state are observed in many ion channels in their “resting” state, but it is seldom clear to what extent such transitions are controlled by an extrinsic modulatory factor. In GIRK channels, one such factor may be the ubiquitously present PIP<sub>2</sub>, which is an obligatory gating factor in these channels (60). Also, it has been proposed that intracellular Na<sup>+</sup> is an important regulatory factor that may substantially regulate  $A_{\text{GIRK,basal}}$  (23, 46). Na<sup>+</sup> may activate GIRK in a Gβγ-dependent manner (61) (this component should be absent in oocytes expressing the Gβγ scavengers) and also via a direct binding (23). The  $\text{EC}_{50}$  of the direct Na<sup>+</sup> effect is 20–30 mM (62), and the extent of direct activation is probably minor in resting cells, at physiological Na<sup>+</sup> concentrations of 5–10 mM. Further studies will be necessary to clarify whether a Gβγ-independent component of  $A_{\text{GIRK,basal}}$  exists and what is the underlying mechanism.

**Acknowledgments**—We thank E. Peralta, P. Hartig, P. Kofuji, E. Reuveny, R. J. Lefkowitz, and M. Lohse for kindly providing cDNA clones; C. W. Dessauer for the generous gift of purified G protein subunits; and I. Lotan and T. Ivanina for insightful comments on the manuscript.

## REFERENCES

- Clapham, D. E., and Neer, E. J. (1997) *Annu. Rev. Pharmacol. Toxicol.* **37**, 167–203
- Dascal, N. (1997) *Cell Signal.* **9**, 551–573
- Stanfield, P. R., Nakajima, S., and Nakajima, Y. (2003) *Rev. Physiol. Biochem. Pharmacol.* **145**, 47–179
- Kurachi, Y., and Ishii, M. (2004) *J. Physiol. (Lond.)* **554**, 285–294
- Logothetis, D. E., and Zhang, H. (1999) *J. Physiol. (Lond.)* **520**, 630
- Hilgemann, D. W., Feng, S., and Nasuhoglu, C. (2001) *Science's STKE* [http://www.stke.org/cgi/content/full/OC\\_sigtrans;2001/111/re19](http://www.stke.org/cgi/content/full/OC_sigtrans;2001/111/re19)
- Ito, H., Ono, K., and Noma, A. (1994) *J. Physiol. (Lond.)* **476**, 55–68
- Torreccilla, M., Marker, C. L., Cintora, S. C., Stoffel, M., Williams, J. T., and Wickman, K. (2002) *J. Neurosci.* **22**, 4328–4334
- Takigawa, T., and Alzheimer, C. (2002) *J. Physiol. (Lond.)* **539**, 67–75
- Luscher, C., Jan, L. Y., Stoffel, M., Malenka, R. C., and Nicoll, R. A. (1997) *Neuron* **19**, 687–695
- Blanchet, C., and Luscher, C. (2002) *Proc. Natl. Acad. Sci. U. S. A.* **99**, 4674–4679
- Sharon, D., Vorobiov, D., and Dascal, N. (1997) *J. Gen. Physiol.* **109**, 477–490
- Kobrinsky, E., Mirshahi, T., Zhang, H., Jin, T., and Logothetis, D. E. (2000) *Nat. Cell Biol.* **2**, 507–514
- Meyer, T., Wellner-Kienitz, M. C., Biewald, A., Bender, K., Eickel, A., and Pott, L. (2000) *J. Biol. Chem.* **276**, 5650–5658
- Leaney, J., Dekker, L., and Tinker, A. (2001) *J. Physiol. (Lond.)* **534**, 367–379
- Lei, Q., Talley, E. M., and Bayliss, D. A. (2001) *J. Biol. Chem.* **276**, 16720–16730
- Reuveny, E., Slesinger, P. A., Inglese, J., Morales, J. M., Iniguez-Lluhi, J. A., Lefkowitz, R. J., Bourne, H. R., Jan, Y. N., and Jan, L. Y. (1994) *Nature* **370**, 143–146
- Vivaudou, M., Chan, K. W., Sui, J. L., Jan, L. Y., Reuveny, E., and Logothetis, D. E. (1997) *J. Biol. Chem.* **272**, 31553–31560
- Petit-Jacques, J., Sui, J. L., and Logothetis, D. E. (1999) *J. Gen. Physiol.* **114**, 673–684
- Peleg, S., Varon, D., Ivanina, T., Dessauer, C. W., and Dascal, N. (2002) *Neuron* **33**, 87–99
- Ivanina, T., Rishal, I., Varon, D., Mullner, C., Frohnwieser-Steinecke, B., Schreibmayer, W., Dessauer, C. W., and Dascal, N. (2003) *J. Biol. Chem.* **278**, 29174–29183
- Zhang, Q., Pacheco, M. A., and Doupnik, C. A. (2002) *J. Physiol. (Lond.)* **545**, 355–373
- Sui, J. L., Chan, K. W., and Logothetis, D. E. (1996) *J. Gen. Physiol.* **108**, 381–391
- Ho, I. H., and Murrell-Lagnado, R. D. (1999) *J. Biol. Chem.* **274**, 8639–8648
- Zhang, H., He, C., Yan, X., Mirshahi, T., and Logothetis, D. E. (1999) *Nat. Cell Biol.* **1**, 183–188
- Slesinger, P. A., Reuveny, E., Jan, Y. N., and Jan, L. Y. (1995) *Neuron* **15**, 1145–1156
- Huang, C. L., Slesinger, P. A., Casey, P. J., Jan, Y. N., and Jan, L. Y. (1995) *Neuron* **15**, 1133–1143
- Ivanina, T., Varon, D., Peleg, S., Rishal, I., Porozov, Y., Dessauer, C. W., Keren-Raifman, T., and Dascal, N. (2004) *J. Biol. Chem.* **279**, 17260–17268
- Jing, J., Chikvashvili, D., Singer-Lahat, D., Thornhill, W. B., Reuveny, E., and Lotan, I. (1999) *EMBO J.* **18**, 1245–1256
- Blackmer, T., Larsen, E. C., Takahashi, M., Martin, T. F., Alford, S., and Hamm, H. E. (2001) *Science* **292**, 293–297
- Yevenes, G. E., Peoples, R. W., Tapia, J. C., Parodi, J., Soto, X., Olate, J., and Aguayo, L. G. (2003) *Nat. Neurosci.* **6**, 819–824
- Vorobiov, D., Bera, A. K., Keren-Raifman, T., Barzilai, R., and Dascal, N. (2000) *J. Biol. Chem.* **275**, 4166–4170
- Liman, E. R., Tytgat, J., and Hess, P. (1992) *Neuron* **9**, 861–871
- Dascal, N., Doupnik, C. A., Ivanina, T., Bausch, S., Wang, W., Lin, C., Garvey, J., Chavkin, C., Lester, H. A., and Davidson, N. (1995) *Proc. Natl. Acad. Sci. U. S. A.* **92**, 6758–6762
- Dascal, N., and Lotan, I. (1992) in *Protocols in Molecular Neurobiology* (Longstaff, A., and Revest, P., eds) Vol. 13, pp. 205–225, Humana Press, Totowa, NJ
- Schreibmayer, W., Lester, H. A., and Dascal, N. (1994) *Pflugers Arch. Eur. J. Physiol.* **426**, 453–458
- Singer-Lahat, D., Dascal, N., Mittelman, L., Peleg, S., and Lotan, I. (2000) *Pflugers Arch. Eur. J. Physiol.* **440**, 627–633
- Pitcher, J. A., Freedman, N. J., and Lefkowitz, R. J. (1998) *Annu. Rev. Biochem.* **67**, 653–692
- Carman, C. V., Barak, L. S., Chen, C., Liu-Chen, L. Y., Onorato, J. J., Kennedy, S. P., Caron, M. G., and Benovic, J. L. (2000) *J. Biol. Chem.* **275**, 10443–10452
- Nikolov, E. N., and Ivanova-Nikolova, T. T. (2004) *J. Biol. Chem.* **279**, 23630–23636
- Kunkel, M. T., and Peralta, E. G. (1995) *Cell* **83**, 443–449
- Dolphin, A. C. (1998) *J. Physiol. (Lond.)* **506**, 3–11
- Schulz, R. (2001) *Pharmacol. Res.* **43**, 1–10
- Bauer, P. H., Bluml, K., Schroder, S., Hegler, J., Dees, C., and Lohse, M. J. (1998) *J. Biol. Chem.* **273**, 9465–9471
- Kovoor, A., Henry, D. J., and Chavkin, C. (1995) *J. Biol. Chem.* **270**, 589–595
- Vorobiov, D., Levin, G., Lotan, I., and Dascal, N. (1998) *Pflugers Arch. Eur. J. Physiol.* **436**, 56–68
- Savage, J. R., McLaughlin, J. N., Skiba, N. P., Hamm, H. E., and Willardson, B. M. (2000) *J. Biol. Chem.* **275**, 30399–30407
- Kim, C. M., Dion, S. B., and Benovic, J. L. (1993) *J. Biol. Chem.* **268**, 15412–15418
- Sarvazyan, N. A., Remmers, A. E., and Neubig, R. R. (1998) *J. Biol. Chem.* **273**, 7934–7940
- Ross, E. M. (1995) *Recent Prog. Horm. Res.* **50**, 207–221
- Kenakin, T. (2004) *Mol. Pharmacol.* **65**, 2–11
- Rebois, R. V., and Hebert, T. E. (2003) *Receptors Channels* **9**, 169–194
- Hille, B. (1992) *Neuron* **9**, 187–195
- Prybylowski, K., and Wenthold, R. J. (2004) *J. Biol. Chem.* **279**, 9673–9676
- Ruiz-Velasco, V., and Ikeda, S. R. (1998) *J. Physiol. (Lond.)* **513**, 761–773
- Yakubovich, D., Rishal, I., and Dascal, N. (2005) *J. Mol. Neurosci.* **25**, 7–19
- He, C., Zhang, H., Mirshahi, T., and Logothetis, D. E. (1999) *J. Biol. Chem.* **274**, 12517–12524
- He, C., Yang, X., Zhang, H., Mirshahi, T., Jin, T., Huang, A., and Logothetis, D. E. (2002) *J. Biol. Chem.* **277**, 6088–6096
- Finley, M., Arrabit, C., Fowler, C., Suen, K. F., and Slesinger, P. A. (2004) *J. Physiol. (Lond.)* **555**, 643–657
- Mirshahi, T., Jin, T., and Logothetis, D. E. (2003) *Science's STKE* [http://stke.sciencemag.org/cgi/content/full/OC\\_sigtrans;2003/194/pe32](http://stke.sciencemag.org/cgi/content/full/OC_sigtrans;2003/194/pe32)
- Rishal, I., Keren-Raifman, T., Yakubovich, D., Ivanina, T., Dessauer, C. W., Slepak, V. Z., and Dascal, N. (2003) *J. Biol. Chem.* **278**, 3840–3845
- Ho, I. H., and Murrell-Lagnado, R. D. (1999) *J. Physiol. (Lond.)* **520**, 645–651